Macromolecules

pubs.acs.org/Macromolecules Article

Rational Polymer Design of Stretchable Poly(ionic liquid) Membranes for Dual Applications

Bingrui Li, Sheng Zhao, Jiadeng Zhu, Sirui Ge, Kunyue Xing, Alexei P. Sokolov, Tomonori Saito,* and Peng-Fei Cao*

Cite This: *Macromolecules* 2021, 54, 896–905 Read Online

ACCESS | Metrics & More | Article Recommendations | Supporting Information

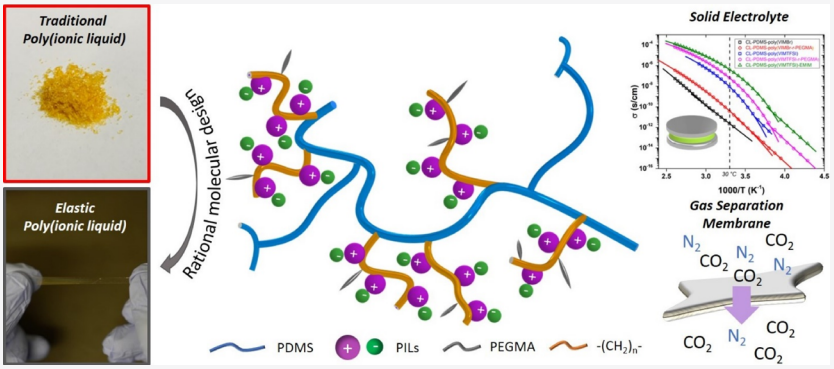

ABSTRACT: Many functional polymeric materials are inherently fragile at ambient conditions. Making them elastic and flexible is a challenging task, and such achievement is especially meaningful in a wide range of applications including separation membranes and stretchable devices. Poly(ionic liquids) (PILs), such as vinyl-imidazolium-based polymers, are known to be "brittle" functional polymers due to their "glassy" nature at ambient temperature. We herein developed a viable approach to enable glassy PILs with high flexibility and good elasticity via a rational molecular design of chemical composition and polymer architectures. The reversible addition/fragmentation chain transfer agents (RAFT-CTAs) were attached to the flexible poly(dimethylsiloxane) (PDMS) backbones. The polymerization of functional ionic liquid monomers from RAFT-CTAs provided grafted copolymers with the functional side chains, which were further cross-linked by di-functional PDMS. Poly(ethylene glycol) methacrylate is copolymerized with ionic liquid monomers to reduce the glass transition temperature (T_g), providing higher chain mobility and elasticity at ambient temperature. The synthesized elastic PIL-based membranes (E-PILs) have dramatically improved stretchability, reaching 122−422%. In addition to significantly improved extensibility, the synthesized E-PILs also exhibit higher ionic conductivity, critical for potential applications in solid-state batteries. Moreover, in comparison to glassy solid PIL membranes, the E-PILs also exhibited enhanced flexibility and excellent gas-separation performance.

INTRODUCTION

Stretchable functional materials capable of retaining functionality under elongation or other physical deformations can be utilized in a wide range of applications such as epidermal electronics,[1,2] sensors,[3−5] electric actuators,[6,7] and medical implants.[8] In comparison to rigid "hard" materials, such as metallic, ceramic, and other inorganic materials, polymeric materials possess intrinsic flexibility and potential extensibility, enabling to serve as attractive building blocks in the fabrication of stretchable functional materials.[9−11] Various repeating subunits of polymers can be programmed in different aspects to embrace the requirements of stretchable functional materials.[12] One straightforward strategy is physically adhering the functional motifs to the stretchable polymer layers.[13−15] Although this approach has a simple implementation, the performance of composite materials depends strongly on the adhesion force between different layers, limiting options of building blocks and widespread use in various applications. A physical blending of a polymer with strong physical interactive groups as a binder for a non-extensible functional unit can also provide a functional material with high stretchability.[16,17] Aside from the physical approach, the strategy of covalently bonding distinctively different building units in one polymer chain can also create polymers with intrinsically dual properties.[18] For example, Liu et al. fabricated a stretchable, electrically

Received: October 14, 2020
Revised: December 9, 2020
Published: December 23, 2020

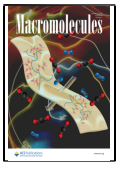

https://dx.doi.org/10.1021/acs.macromol.0c02335
Macromolecules 2021, 54, 896−905

Scheme 1. Demonstration of the Synthetic Route of E-PILs with CL-PDMS-poly(VIMBr-*r*-PEGMA) as a Typical Example. Inset is the Monomer Options as the Polymer Side Chains; Monomer Number Corresponds to the Sample Number in Tables 1 and 2

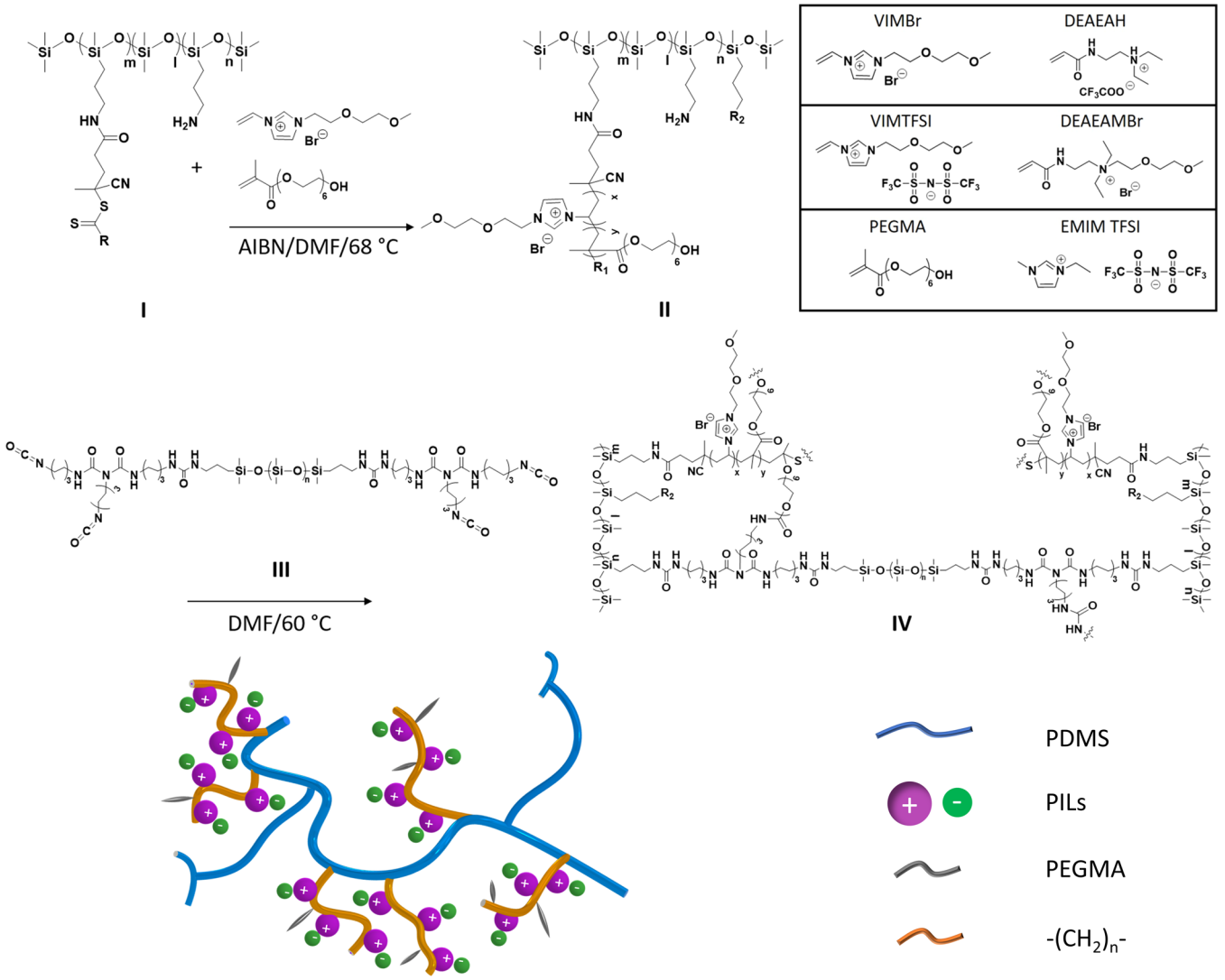

conductive block copolymer in which the polyurethane segment provides extensibility and the poly(3-alkylthiophenes) block provides conductivity.[19] Stretchable semiconductors have also been developed by adopting a similar copolymerization approach via a combination of conjugated semiconducting polymers and non-conjugated moieties that provide hydrogen bonding interactions.[20] Stretchable gas separation membranes obtained by chemical cross-linking of the flexible poly(dimethylsiloxane) (PDMS) chain with the poly(ethylene glycol) (PEG) segments that provide high gas selectivity of CO_2/N_2 were also reported.[21] Despite numerous efforts devoted to developing stretchable functional polymeric materials,[22,23] achieving excellent elasticity of traditionally non-flexible functional materials remains a significant challenge.

Polymerized ionic liquids (PILs) are a family of functional polymeric materials with ionic liquid groups covalently attached to a polymer backbone, i.e., pendant PILs,[24] or covalently connected to form a functional polymer chain, i.e., backbone PILs.[25] Numerous options of ionic liquid units along with different polymer architectures enable PILs with different physical and chemical properties that can satisfy multiple applications. PILs are widely utilized in energy harvesting and storage applications, e.g., acting as solid or gel electrolytes for batteries[26−28] and ionic conducting membranes for anion-exchange fuel cells.[29] A variety of PILs have been demonstrated as highly effective gas capture media[30] and gas separation membranes with enhanced selectivity.[31,32] Moreover, PILs are utilized to produce "smart" materials based on their responsive behavior[33,34] or catalysts for cycloaddition of CO_2 due to their charge features and high solvent compatibility.[35,36] While many efforts were devoted to achieving stretchable PIL-based gels,[37] the solvent-free solid PILs are typically brittle and possess low flexibility.[38] Till now, the solid PILs with high elasticity have rarely been reported. Such achievement will widen their practical applications, especially in the area of attachable devices and separation membranes where flexibility and extensibility can improve their overall performance.

The strategies of developing stretchable functional materials can be adapted to address the brittleness issues of solid PILs and facilitate broader applications. We herein report a rational

https://dx.doi.org/10.1021/acs.macromol.0c02335
Macromolecules 2021, 54, 896−905

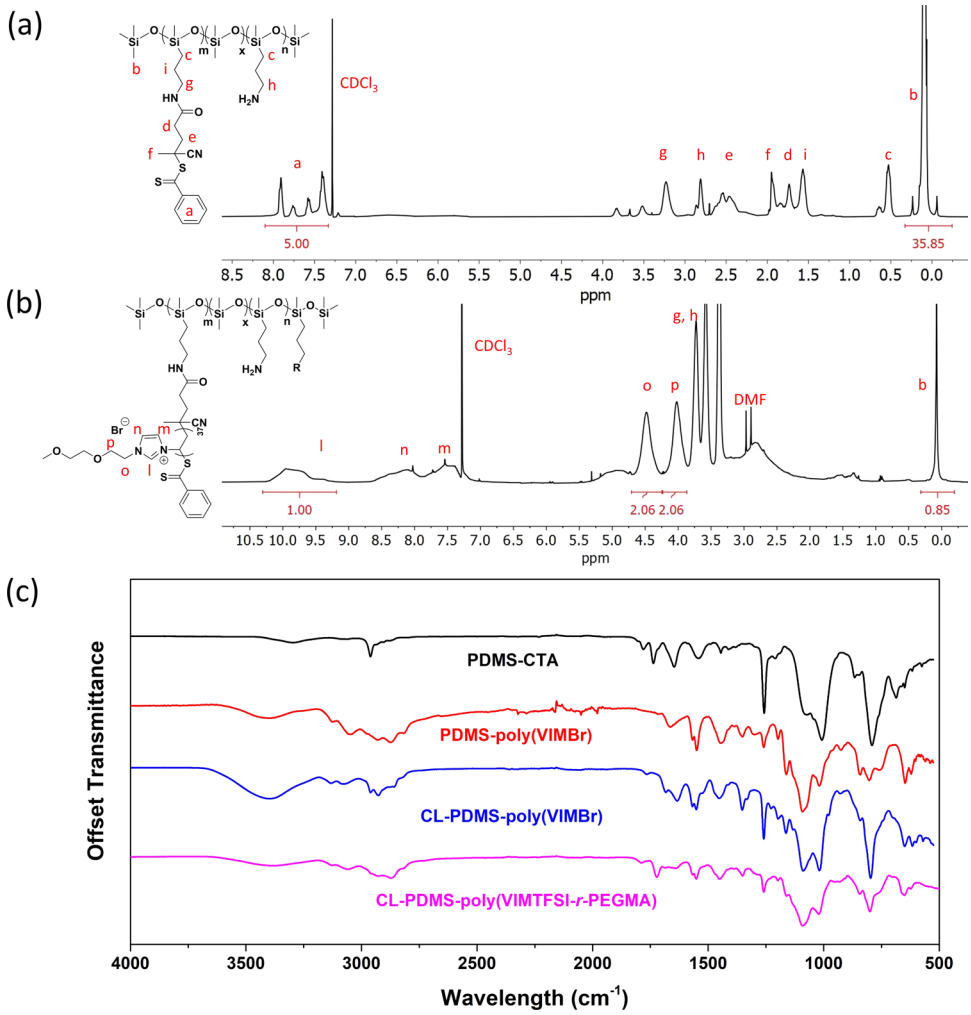

Figure 1. (a) ^{1}H NMR of PDMS-CTA. (b) ^{1}H NMR of PDMS-poly(VIMBr). (c) ATR spectra of PDMS-CTA, PDMS-poly(VIMBr), CL-PDMS-poly(VIMBr) (sample 1), and CL-PDMS-poly(VIMTFSI-*r*-PEGMA) (sample 4).

design of stretchable and elastic solid polymerized ionic liquids (E-PILs) constructed from chemically grafting PIL side chains to a PDMS backbone with an elastic PDMS linker. The PDMS allows the mechanical robustness and extensibility while the grafted PILs provide functionality (ionic conductivity and enhanced gas selectivity). The E-PILs are anticipated to play an important role in flexible sensors, stretchable batteries, and gas separation membranes. The modular strategy is highly versatile for developing other stretchable functional polymers via grafting different types of functional species.

RESULTS AND DISCUSSION

Synthesis of Elastic PILs. Imidazolium and ammonium-based poly(ionic liquid)s are the two widely utilized PIL species that can serve as solid electrolytes,[26] gas sorption/separation materials,[31,39] and desalination membranes.[40] Herein, both types of poly(ionic liquid)s were synthesized starting from the two monomer precursors: 1-vinylimidazole (VIM) and *N*-(2-(diethylamino)ethyl)acrylamide (DEAEA), where DEAEA was synthesized from the nucleophilic addition reaction between acryloyl chloride and *N*,*N*-diethylethylenediamine. The imidazolium-type monomer with bromide as a counterion, i.e., VIMBr, was synthesized from Menshutkin reaction between 1-bromo-2-(2-methoxyethoxy)ethane and 1-vinylimidazole. As illustrated by the ^{1}H NMR spectra of monomers VIMBr and DEAEA in Figure S1, the presence of the peaks f to j from 3.0 to 4.6 ppm indicates the successful attachment of 1-bromo-2-(2-methoxyethoxy)ethane on the VIMBr monomer (Figure S1a), and the peaks at 1.0 (a) and 2.5 ppm (b) suggest the successful nucleophilic addition in DEAEA synthesis (Figure S1b). The VIMTFSI monomer was obtained from the counterion exchange of VIMBr using an excess of bis(trifluoromethane)sulfonimide lithium salt in an aqueous solution. The ammonium-based monomers DEAEAH and DEAEAMBr (Scheme 1) were synthesized from the acidification or quaternization of DEAEA monomer by trifluoroacetic acid or 1-bromo-2-(2-methoxyethoxy)ethane, respectively.

Molecular architecture and chemical composition are designed to achieve elastic PILs. Considering the "glassy" nature of regular imidazolium- and ammonium-based PILs at ambient temperature, PDMS was selected as the polymer backbone due to the ideal material characteristics such as a highly flexible Si−O bond, low glass-transition temperature (T_g ≈ −123 °C), and good thermal stability.[41−46] Among the numerous polymer architectures, grafted copolymers is especially attractive due to their capability to provide relatively independent roles for polymer backbone and grafted side chains.[47] Thus, the polymerized ionic liquids were grafted onto the PDMS backbone as the side chains, and chemical cross-

https://dx.doi.org/10.1021/acs.macromol.0c02335
Macromolecules 2021, 54, 896−905

Table 1. Combined Chemical, Thermal, and Rheological Properties of PIL Membranes

sample no.	sample name	$T_{d,5\%}$ (°C)	T_g (°C)	density (g/cm^3)	G' (Pa)	cross-link density (mol/cm^3)
1	CL-PDMS-poly(VIMBr)	248	51.6	1.40	1.48×10^4	4.07×10^{-4}
2	CL-PDMS-poly(VIMBr-*r*-PEGMA)	266	19.7	1.35	4.88×10^4	1.34×10^{-5}
3	CL-PDMS-poly(VIMTFSI)	275	24.4	1.42	4.59×10^4	1.26×10^{-5}
4	CL-PDMS-poly(VIMTFSI-*r*-PEGMA)	307	9.2	1.51		
5	CL-PDMS-poly(VIMTFSI)-EMIM	328	−8.2	1.52	3.79×10^3	1.04×10^{-6}
6	CL-PDMS-poly(DEAEAH)	207	26.6	1.24	4.88×10^4	1.34×10^{-5}
7	CL-PDMS-poly(DEAEAH-*r*-PEGMA)	215	10.1	1.29		
8	CL-PDMS-poly(DEAEAMBr)	246	35.1	1.28	4.30×10^4	1.18×10^{-5}
9	CL-PDMS-poly(DEAEAMBr-*r*-PEGMA)	235	8.0	1.25	8.17×10^4	2.25×10^{-5}

Table 2. Tensile Test Data of PIL Membranes

sample no.	sample name	Young's modulus (MPa)	elongation at break (%)	toughness (MJ/m^3)	ultimate tensile stress (MPa)
1	CL-PDMS-poly(VIMBr)	320.4	0.4	0.004	1.5
2	CL-PDMS-poly(VIMBr-*r*-PEGMA)	1.1	122.5	0.04	0.6
3	CL-PDMS-poly(VIMTFSI)	15.3	5.8	0.02	0.5
4	CL-PDMS-poly(VIMTFSI-*r*-PEGMA)	1.3	422.7	1.8	0.8
5	CL-PDMS-poly(VIMTFSI)-EMIM	0.5	164.7	0.5	0.5
6	CL-PDMS-poly(DEAEAH)	4.5	5.3	0.05	0.1
7	CL-PDMS-poly(DEAEAH-*r*-PEGMA)	0.1	226.1	0.1	0.07
8	CL-PDMS-poly(DEAEAMBr)	0.4	5.3	0.2	5.2
9	CL-PDMS-poly(DEAEAMBr-*r*-PEGMA)	0.9	133.4	0.2	0.2

linking was performed to bridge the grafted polymers via difunctionalized PDMS. This architecture not only preserves the functionalities of PILs but also offers tunability toward different types of PILs within a stretchable PDMS network targeting different applications.

The PDMS possessing numerous amine groups (PDMS-NH_2, 20,000 g/mol, ~48 $-NH_2$ groups per molecule as calculated from the ^{1}H NMR spectrum in Figure S2) was chemically modified with a chain transfer agent (CTA) as shown in Scheme 1 (compound I, PDMS-CTA), and the ^{1}H NMR result indicates the attachment of ~36 CTAs on one chain of PDMS-NH_2. Reversible addition−fragmentation chain-transfer (RAFT) polymerizations were performed to grow the PILs as the side chains of the grafted copolymers. It should be noticed that from the macro RAFT-CTA, i.e., PDMS-CTA, different types of ionic liquid monomers can be utilized to obtain different types of grafted copolymers including PDMS-poly(VIMBr), PDMS-poly(VIMTFSI), PDMS-poly(DEAEAH), and PDMS-poly(DEAEAMBr). As illustrated by the ^{1}H NMR spectra of PDMS-poly(VIMBr) in Figure 1b, the appearance of proton signals (peaks o and p) in the poly(imidazolium) structure indicated the successful RAFT polymerization of VIMBr on the side chain of PDMS by comparing the integration of peak o at 4.5 ppm with peak b at 0 ppm (Figure 1b), the degree of polymerization (DP_n) for each CTA was calculated to be 36. The significant broad peak at approximately 3400 cm^{-1} in the attenuated total reflection Fourier-transform infrared (ATR FTIR) spectra corresponds to the N−H stretch, which also confirms the presence of a large amount of poly(VIMBr) in the obtained grafted copolymer (Figure 1c). The chemical structure of elastic cross-linker is shown in Scheme 1(compound III), and the molar ratio between grafted copolymer (compound II) and PDMS cross-linker is fixed at 1:12. The polymer solution was cast into a PTFE dish and dried, resulting in a cross-linked graft copolymer (compound IV). The detailed synthesis procedures are described in the experimental section of the Supporting Information. In the ATR FTIR spectra of CL-PDMS-poly(VIMBr), the further intensity increase of the N−H stretching peak at around 3400 cm^{-1} in comparison to the PDMS-poly(VIMBr) indicates the formation of more urea units. Considering the good water solubility of PDMS-poly(VIMBr), the insolubility of CL-PDMS-poly(VIMBr) in types of solvents also confirms the cross-linked nature.

The physical properties of the synthesized PIL-based membranes are summarized in Table 1. All PIL-based films exhibit thermal stability higher than 200 °C with less than 5% weight loss in the thermogravimetric analysis (see Figure S3), which should satisfy the typical application temperature range of solid-state electrolyte.[48] However, all of the prepared membranes with only PILs as the side chain, CL-PDMS-poly(VIMTFSI), CL-PDMS-poly(DEAEAH), and CL-PDMS-poly(DEAEAMBr), i.e., samples 3, 6, and 8 in Table 1, respectively, suffered from mechanical fragility and were non-extensible (Table 2). Differential scanning calorimetry (DSC) analysis (Figure 2 and Figure S4) revealed that the glass transition temperature (T_g) of these PILs (samples 1, 3, 6, and 8 in Table 1) is above 24 °C, indicating the glassy state of these polymer membranes at ambient temperature. As an example, sample 1, CL-PDMS-poly(VIMBr), shows $T_g \approx 51.6$ °C, consistent with previously reported linear poly(*N*-vinyl diethylene glycol ethyl methyl ether imidazolium bromide), with a T_g of 75 °C.[49] A slightly lower T_g value of the current system can be explained by the presence of low-T_g PDMS as the backbone and cross-linker, which can increase the chain mobility.[49,50]

As an initial attempt to lower the T_g of obtained PIL-based membranes, the IL-monomer with larger counter ions, i.e., VIMTFSI and DEAEAH (see Scheme 1 for chemical structure), have been synthesized, following the same protocols. The ionic liquid with larger counter ions was reported to exhibit a lower T_g due to the weaker ion associations.[32,49] However, while CL-PDMS-poly(VIMTFSI) (sample 3) and CL-PDMS-poly(DEAEAH) (sample 6)

https://dx.doi.org/10.1021/acs.macromol.0c02335
Macromolecules 2021, 54, 896−905

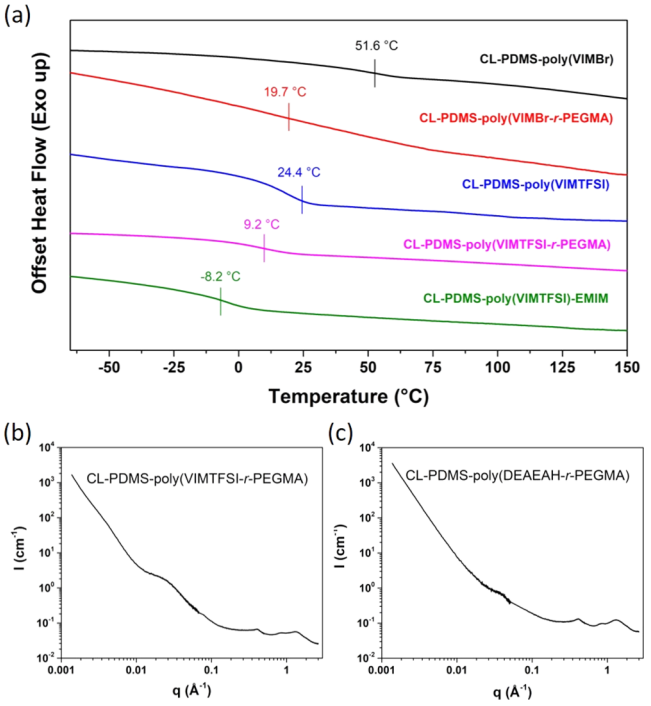

Figure 2. (a) DSC data of selected PIL membranes. (b) SAXS-WAXS data of CL-PDMS-poly(VIMTFSI-*r*-PEGMA). (c) SAXS-WAXS data of CL-PDMS-poly(DEAEAH-*r*- PEGMA).

exhibits lower T_g values (T_g = 24.4 and 26.6 °C for samples 3 and 6, respectively) in comparison to CL-PDMS-poly(VIMBr) (sample 1, 51.6 °C) and CL-PDMS-poly(DEAEAMBr) (sample 8, 35.1 °C), these two PIL membranes with larger counterions were still in a glassy state at ambient temperature. Therefore, only increasing the size of counterions in PIL-based membranes did not significantly improve their extendibility, as shown in Table 2 (strain at break for sample 3 = 5.82% and strain at break for sample 6 = 5.32%).

Being compatible with other monomers in the copolymerization,[51] PEG has been widely utilized to lower the T_g for multi-component systems.[52] Therefore, starting from the PDMS-CTA, random copolymerizations of ionic liquid monomers with PEG methacrylate (PEGMA) were performed followed by a cross-linking reaction. The obtained membranes were named as CL-PDMS-poly(VIMBr-*r*-PEGMA) (sample 2), CL-PDMS-poly(VIMTFSI-*r*-PEGMA) (sample 4), CL-PDMS-poly(DEAEAH-*r*-PEGMA) (sample 7), and CL-PDMS-poly(DEAEAMBr-*r*-PEGMA) (sample 9), whose chemical composition and physical properties are listed in Table 1. With over 20 wt % of PEGMA, the T_g value of obtained membranes is significantly lower than those without PEG. Moreover, random copolymerization of ionic liquids and PEG monomers helps to separate ionic pairs in the PIL segments and results in low electrostatic interactions, which should also contribute to lowering the T_g of the resulting system.[53]

The significantly lower T_g values in all PILs (around 15−30 °C decrease, see Figure 2 and Table 1) due to the incorporation of PEGMA ensures the polymers being in a "rubbery" state instead of a glassy state at room temperature (T_g of PEGMA containing samples: 8 and 19.7 °C for samples 9 and 2, respectively). The presence of only one glass transition process from DSC data of PEGMA-containing samples (Figure 2a) demonstrated the absence of a significant phase separation after the incorporation of PEGMA. This is confirmed by their small angle X-ray scattering (SAXS) spectra (Figure 2b,c, Figure S7). The broad peak with q values from 0.01 to 0.03 Å^{-1} in the SAXS spectrum is attributed to the formation of nanoclusters introduced by RAFT-CTA under the driving force of hydrophobic interactions.[54] The increased molecular mobility in PEG-containing PILs, such as the samples 2 and 9, should achieve significantly improved extensibility, and this "softening" effect introduced by the PEG is consistent with previous reports.[55,56]

Mechanical Properties of PIL Membranes. Rheological tests were conducted to evaluate the segmental dynamic and cross-link density of the PILs. Master curves were obtained by conducting frequency sweep at different temperatures followed by a temperature−frequency superposition at a reference temperature. The spectra of G'' show usual behavior for slightly (or non-) entangled polymers with low cross-linking density. The segmental relaxation time τ_α was calculated from the angular frequency ω_s corresponding to the crossover of storage modulus (G') and loss modulus (G'') in a high-frequency range as follows:[57]

$$\tau_\alpha = \frac{1}{\omega_s} \tag{1}$$

The results demonstrate significantly shorter segmental relaxation time after the incorporation of PEGMA in comparison to membranes with only PIL as a sidechain. For example, the segmental relaxation time of CL-PDMS-poly(VIMTFSI-*r*-PEGMA) (sample 4) is reduced by four orders in comparison to CL-PDMS-poly(VIMTFSI) (sample 3) at the same temperature.

The plateau region at a lower frequency (equivalent to measurement at a higher) of the storage modulus G' curves of obtained films indicates the cross-linked structure, and the cross-linking density (c_x) can be estimated from this plateau value (Figure 3a−d, Figure S5a,b) by the following equation[58]

$$c_x = \frac{2G'}{3RT} = \frac{2\rho}{3M_x} \tag{2}$$

where c_x is the moles of cross-links per volume, ρ is polymer density, M_x is the number-average molecular weight between the cross-links, G' is the plateau value of shear modulus (Figure 3a−d), R is the gas constant, and T is the temperature in Kelvin. The calculated values are shown in Table 1, whereas the c_x of the CL-PDMS-poly(VIMTFSI-*r*-PEGMA) and CL-PDMS-poly(DEAEAH-*r*-PEGMA) membranes cannot be calculated due to the difficulty in detecting the modulus plateau. We also prepared CL-PDMS-poly(VIMTFSI)-EMIM (sample 5) by incorporating 30 wt % of ionic liquid (EMIM-TFSI) into CL-PDMS-poly(VIMTFSI) (sample 4) due to their potentially improved performance as solid electrolyte and gas-separation membranes,[59] which will be discussed later. By comparing the G' plateau values of CL-PDMS-poly(VIMTFSI) (sample 3) and CL-PDMS-poly(VIMTFSI)-EMIM (sample 5), it was observed that the addition of EMIM-TFSI ionic liquid resulted in a lower G' value and reduced cross-linking density. Comparison of CL-PDMS-poly(VIMBr) to CL-PDMS-poly(VIMBr-*r*-PEGMA) and CL-PDMS-poly(DEAEAMBr) to CL-PDMS-poly(DEAEAMBr-*r*-PEGMA) reveals a higher cross-linking density in PEG-incorporated samples than in the PEG-free samples. This can

https://dx.doi.org/10.1021/acs.macromol.0c02335
Macromolecules 2021, 54, 896−905

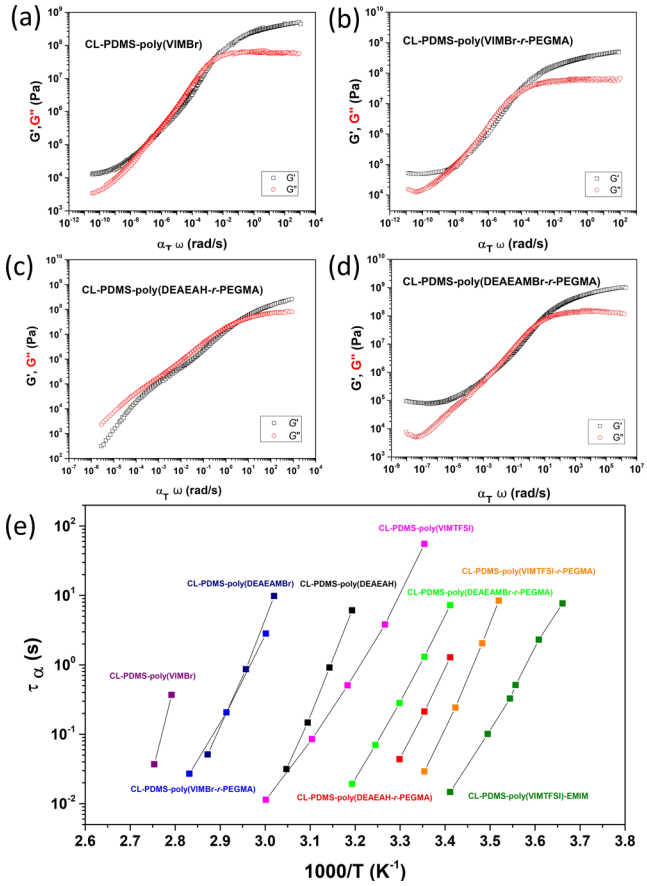

Figure 3. Shear modulus (reference temperature = 30 °C) of (a) CL-PDMS-poly(VIMBr), (b) CL-PDMS-poly(VIMBr-*r*-PEGMA), (c) CL-PDMS-poly(DEAEAH-*r*-PEGMA), and (d) CL-PDMS-poly-(DEAEAMBr-*r*-PEGMA). (e) Temperature dependence of the segmental relaxation time in studied PILs.

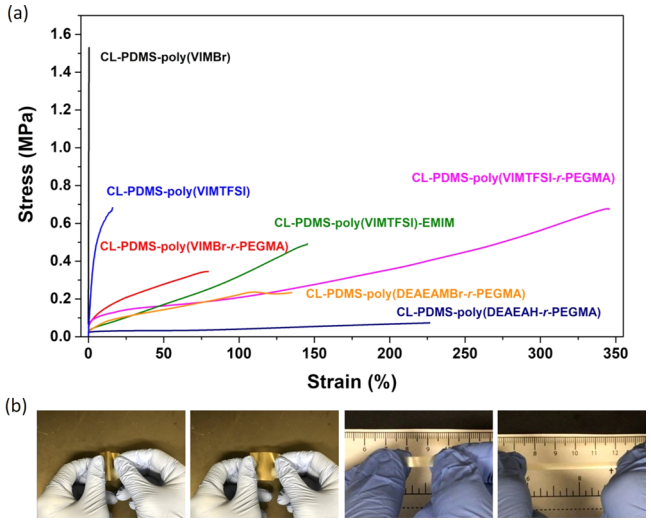

Figure 4. (a) Tensile test data of PILs. (b) Photos of CL-PDMS-poly(VIMTFSI-*r*-PEGMA).

be explained by the fact that the −OH terminal group in the PEG readily reacts with the isocyanate-terminated PDMS cross-linker forming a urethane group, resulting in higher chemical cross-linking density.

The flexibility and extensibility of CL-PDMS-poly-(VIMTFSI-r-PEGMA) (sample 4) are clearly demonstrated (Figure 4b) when it was bent and stretched. Tensile test of the E-PILs was performed by an RSA-G2 solid analyzer, with results shown in Figure 4a and Table 2. As seen in the Figure 4a, the films without copolymerization with PEGMA, i.e., CL-PDMS-poly(VIMBr) (sample 1), CL-PDMS-poly(VIMTFSI) (sample 3), CL-PDMS-poly(DEAEAH) (sample 6), and CL-PDMS-poly(DEAEAMBr) (sample 8), exhibited high modulus, high tensile stress, and low elongation-at-break: sample 1 shows elongation-at-break of only 0.40% with a Young's modulus of 320 MPa; samples 3, 6, and 8 show similar tensile behavior with an elongation-at-break of less than 6%. As expected, the effect of PEG incorporation is dramatic for these PIL-based membranes, and with only 25% molar ratio, the films with copolymerization of PEG, i.e., CL-PDMS-poly-(VIMBr-*r*-PEGMA) (sample 2), CL-PDMS-poly(VIMTFSI-*r*-PEGMA) (sample 4), CL-PDMS-poly(DEAEAH-*r*-PEGMA) (sample 7), and CL-PDMS-poly(DEAEAMBr-*r*-PEGMA) (sample 9) showed around 20 times higher extensibility than those PIL-based films without PEG. For example, CL-PDMS-poly(VIMBr-*r*-PEGMA) exhibits an elongation-at-break of 423% and a Young's modulus of 1.3 MPa (Table 2). This mechanical performance should satisfy the requirement of a stretchable material in a flexible electronic device.[3] The improved extensibility is caused by the significantly lower T_g value: 19.7 °C for CL-PDMS-poly(VIMBr-*r*-PEGMA) versus 51.6 °C for CL-PDMS-poly(VIMBr), which enables the transition from a glassy to a rubbery state, and increased chain flexibility.

Moreover, comparison of the ionic liquid-doped membrane, i.e., CL-PDMS-poly(VIMTFSI)-EMIM (sample 5), to the CL-PDMS-poly(VIMTFSI-*r*-PEGMA) (sample 4) revealed both higher modulus (1.29 vs 0.52 MPa) and improved elongation-at-break (422.7 vs 164.7%) in the latter case, clearly demonstrating the advantage of the molecular-level-designed intrinsic elastic PILs over the composite elastic PIL. Hysteresis test of the sample 4 was also conducted from 0 to 50% strain for 10 cycles to evaluate its elastic recovery. As seen in Figure S5c, the sample was able to retain 76% of initial stress after 10 cycles, with the overall hysteresis behavior outperforming some polyurethane thermoplastic elastomers.[60] We also observed minimal stress decay after 5 cycles, and the stress value intends to be stable at 50 kPa, which indicates good elasticity (>75% initial stress remaining after 10 cycles) of the obtained E-PIL membrane.

Conductivity Evaluation. PILs are promising materials for use in the solid-state electrolyte in batteries, supercapacitors, and other electronics.[23,24] Broadband dielectric spectroscopy (BDS) was utilized to evaluate the ionic conductivity of the PIL-based membranes, with data from the cooling cycle shown in Figure 5 and Figure S6. In all curves, the temperature dependence of conductivity exhibits a transition from a Vogel−Fulcher−Tammann (VFT) behavior to an Arrhenius behavior upon cooling, with the crossover happening around T_g of the sample.[61] The T_g values obtained from the BDS are consistent with those obtained from the DSC (Table 1).

The ionic conductivity of CL-PDMS-poly(VIMTFSI) with $TFSI^-$ counter ion (sample 3) at T = 30 °C is about two orders of magnitude higher than that of the same polymer with Br^- counter ion (CL-PDMS-poly(VIMBr), sample 1). This is explained by lower T_g and faster segmental dynamics. Moreover, in a system with decoupled conductivity, the size

https://dx.doi.org/10.1021/acs.macromol.0c02335
Macromolecules 2021, 54, 896−905

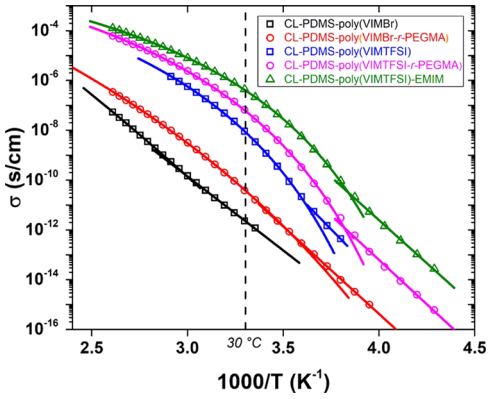

Figure 5. Temperature dependence of conductivity (σ) of samples 1–5.

of free anions will also significantly affect their ionic conductivity,[62,63] and the larger anion in sample 3 will lead to more dissociation of the anion, resulting in improved ionic conductivity.[64] The ionic liquid EMIM-doped membrane CL-PDMS-poly(VIMTFSI)-EMIM exhibited the highest conductivity among all samples, which is mainly attributed to the high concentration of free ionic pairs (EMIM-EFSI) compared to the PILs with only mobile anions. It is worth noticing that the PEG incorporated samples also exhibited higher ionic conductivity than those without PEG due to the faster segmental dynamics rendered by the introduced PEGMA side chain. For example, CL-PDMS-poly(VIMBr-*r*-PEGMA) (sample 2) exhibits over one order higher conductivity than CL-PDMS-poly(VIMBr) (sample 1). With decent ionic conductivity (10^{-6} s/cm) and good mechanical performance, especially high extensibility (423% maximum strain) at ambient temperature (30 °C), sample 4, CL-PDMS-poly(VIMTFSI-*r*-PEGMA), presents high potential to be utilized as a conductive solid polyelectrolyte, whose ionic conductivity can be further tuned by additional ionic liquid and/or inorganic salts.[65]

The present system shows excellent mechanical performance in comparison to the previous literature, i.e., an ultimate tensile stress higher than 1 MPa and a maximum extensibility over 300%, while the ionic conductivity is slightly lower than reported values due to the absence of any additional plasticizers and salts (see Table S1).

We prepared two additional samples that have different molar ratios of VIMTFSI/PEGMA, i.e., CL-PDMS-poly(VIMTFSI-*r*-PEGMA)(45:5) and CL-PDMS-poly(VIMTFSI-*r*-PEGMA)(30:20), and the BDS results are shown in Figure S9. Increasing the molar ratio of PEGMA over the VIMTFSI from VIMTFSI:PEGMA = 45:5 to 30:20 resulted in a slight increase in ion conductivity at 30 °C. This can be explained by the higher chain mobility with increased PEGMA loading, which is verified by the lower T_g. The optimum ratio for achieving the highest ionic conductivity with CL-PDMS-poly(VIMTFSI-*r*-PEGMA) is identified as VIMTFSI:PEGMA = 40:10 (sample 4), which emphasizes the importance of balancing between high $TFSI^-$ ion concentration and low T_g contributed by PEGMA content. We also performed the study on varying the chain length of the PEGMA monomer: a sample with PEGMA of 500 g/mol (3 more PEG repeat units) was prepared. The obtained BDS data (Figure S9) suggest that changing the PEG side chain length shows a similar effect to the changing molar ratio of the PEGMA.

To examine the electrochemical stability of E-PIL membranes, liner sweep voltammetry (LSV) was performed on selected samples, as shown in Figure S8. All the measured samples, i.e., CL-PDMS-poly(VIMBr-*r*-PEGMA) (sample 2), CL-PDMS-poly(VIMTFSI-*r*-PEGMA) (sample 4), and CL-PDMS-poly(DEAEAMBr-*r*-PEGMA (sample 9), exhibit excellent voltage stabilities of being above 4.2 V versus Li/Li^+, and sample 4 shows even higher electrochemical stability above 4.8 V versus Li/Li^+. The result suggests that these PIL-based elastic membranes may be used in batteries containing high-voltage electrode.

Gas Separation Performance. PILs have been well-investigated in gas separation membranes due to their potential in improving gas permeation and selectivity for certain gas pairs (CO_2/N_2, CO_2/CH_4, etc.) by tuning solubility and utilizing optimized cation–anion pairs.[59,66] In industrial applications, gas separation membranes are commonly manufactured under a three-layer design: porous support, gutter layer, and selective layer, where the gutter layer serves as an isolation layer as well as a surface roughness modifier.[67] To reduce the complexity, a layer with good mechanical stability, high flexibility, and decent gas permeation properties may play as both the gutter layer and the selective layer. Therefore, the flexibility and stretchability of the developed E-PIL system may be advantageous for this application. To demonstrate their potential application as gas-separation membranes, the gas permeability of E-PIL membranes was measured in a custom-built instrument.[50] The PIL membranes without PEGMA, including CL-PDMS-poly(VIMBr), CL-PDMS-poly(DEAEAH), and CL-PDMS-poly(DEAEAMBr) all failed in the gas-separation tests due to physical rupture caused by the high fragility of membranes when applying pressure difference on two sides of the membrane. All of PEG-incorporated PIL membranes, i.e., CL-PDMS-poly(VIMBr-*r*-PEGMA), CL-PDMS-poly(VIMTFSI-*r*-PEGMA), CL-PDMS-poly(DEAEAH-*r*-PEGMA), and CL-PDMS-poly(DEAEAMBr-*r*-PEGMA), (samples 2, 4, 7, and 9) maintained integrity at the test condition, which also indicates the significant advantage of elastic membranes. With the elastic PDMS backbones providing fast segmental mobility at ambient temperature, ionic liquid,[68] and PEG segments operated as CO_2-philic functional groups,[69] all elastic PILs (samples 2, 4, 7, and 9) exhibit a higher gas permeability and CO_2/N_2 selectivity as shown in Figure 6. Comparison of the gas

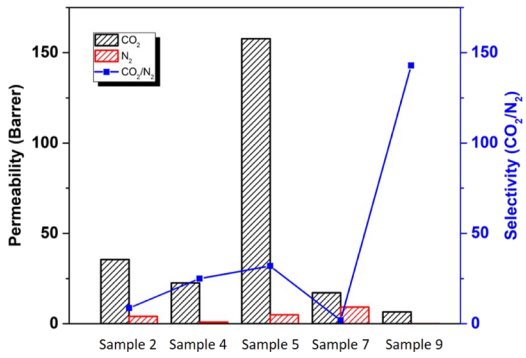

Figure 6. Summary of gas permeation data of E-PIL membranes. Sample 2: CL-PDMS-poly(VIMBr-*r*-PEGMA); sample 4: CL-PDMS-poly(VIMTFSI-*r*-PEGMA); sample 5: CL-PDMS-poly(VIMTFSI)-EMIM; sample 7: CL-PDMS-poly(DEAEAH-*r*-PEGMA); sample 9: CL-PDMS-poly(DEAEAMBr-*r*-PEGMA).

https://dx.doi.org/10.1021/acs.macromol.0c02335
Macromolecules 2021, 54, 896–905

separation performance of samples 2 and 4 (Figure 6) reveals that the sample with $TFSI^-$ counterion shows higher gas permeability than that with Br^- counterion. This can be explained by the faster molecular dynamics in the $TFSI^-$ sample due to the lower T_g, which allows faster gas molecules transport through the membranes. In the ionic liquid-doped PILs, i.e., CL-PDMS-poly(VIMTFSI)-EMIM, the "free" EMIM-TFSI ionic liquid in the system enables efficient interaction between gas and membranes, thus most likely increasing solubility selectivity, which leads to a high CO_2/N_2 selectivity of 32 and decent CO_2 permeability of 158 Barrer. Considering the normally achieved permeation and selectivity values, these samples are considered among the best PIL-based gas separation membranes.[70] The good mechanical stability and versatile molecular design of the membranes indicate great potentials of current membranes for practical applications.

CONCLUSIONS

A series of elastic poly(ionic liquids) membranes were fabricated by growing the copolymer of ionic liquid monomers and PEGMAs as the side chain of PDMS backbones to form grafted copolymers followed by a chemical cross-link using elastic PDMS linkers. Utilization of PDMS as a backbone and a cross-linker, together with the incorporation of PEGMA in the side chain, are the key design to reduce their T_g, achieving a rubbery state at ambient temperature and enabling the elasticity of resulting PIL-based membranes. The obtained E-PIL membranes showed excellent extensibility and reasonable stiffness, a significant improvement over those PIL membranes without PEGMA, even those doped with ionic liquid. BDS analysis revealed that the ionic conductivity of E-PILs can be tuned by introducing different ionic liquid species, copolymerization with PEGMA in the side chain or doped with additional ionic liquid. The E-PIL also exhibited great potential to be utilized as gas-separation membranes, and PEG-incorporated samples demonstrated excellent CO_2/N_2 separation capability along with outstanding structural integrity.

The demonstrated PIL-based membrane with significantly improved elasticity will benefit a wide range of applications, not limited to the gas-separation membrane and energy-storage devices, considering the unique properties of PILs. Moreover, the knowledge gained during this process may shed light on the versatile molecular design of polymeric materials with enhanced mechanical performance and functionalities.

ASSOCIATED CONTENT

Supporting Information

The Supporting Information is available free of charge at https://pubs.acs.org/doi/10.1021/acs.macromol.0c02335.

Experimental section, ^1H NMR spectra, TGA, DSC, rheology, BDS, LSV, and SAXS data (PDF)

AUTHOR INFORMATION

Corresponding Authors

Tomonori Saito − *The Bredesen Center for Interdisciplinary Research and Graduate Education, University of Tennessee, Knoxville, Tennessee 37996, United States; Chemical Sciences Division, Oak Ridge National Laboratory, Oak Ridge, Tennessee 37830, United States;* orcid.org/0000-0002-4536-7530; Email: saitot@ornl.gov

Peng-Fei Cao − *Chemical Sciences Division, Oak Ridge National Laboratory, Oak Ridge, Tennessee 37830, United States;* orcid.org/0000-0003-2391-1838; Email: caop@ornl.gov

Authors

Bingrui Li − *The Bredesen Center for Interdisciplinary Research and Graduate Education, University of Tennessee, Knoxville, Tennessee 37996, United States;* orcid.org/0000-0002-4974-5826

Sheng Zhao − *Department of Chemistry, University of Tennessee, Knoxville, Tennessee 37996, United States*

Jiadeng Zhu − *Chemical Sciences Division, Oak Ridge National Laboratory, Oak Ridge, Tennessee 37830, United States;* orcid.org/0000-0003-4709-4115

Sirui Ge − *Department of Material Science and Engineering, University of Tennessee, Knoxville, Tennessee 37996, United States*

Kunyue Xing − *Department of Chemistry, University of Tennessee, Knoxville, Tennessee 37996, United States;* orcid.org/0000-0002-6948-992X

Alexei P. Sokolov − *Chemical Sciences Division, Oak Ridge National Laboratory, Oak Ridge, Tennessee 37830, United States; Department of Chemistry, University of Tennessee, Knoxville, Tennessee 37996, United States;* orcid.org/0000-0002-8187-9445

Complete contact information is available at: https://pubs.acs.org/10.1021/acs.macromol.0c02335

Notes

The authors declare no competing financial interest.

ACKNOWLEDGMENTS

This study was supported by the U.S. Department of Energy, Office of Science, Basic Energy Sciences, Materials Sciences and Engineering Division. A portion of this research was conducted at the Center for Nanophase Materials Sciences, which is a DOE Office of Science User Facility.

REFERENCES

(1) Koo, J. H.; Kim, D. C.; Shim, H. J.; Kim, T. H.; Kim, D. H. Flexible and Stretchable Smart Display: Materials, Fabrication, Device Design, and System Integration. *Adv. Funct. Mater.* **2018**, *28*, 1801834.

(2) Palleau, E.; Reece, S.; Desai, S. C.; Smith, M. E.; Dickey, M. D. Self-healing stretchable wires for reconfigurable circuit wiring and 3D microfluidics. *Adv. Mater.* **2013**, *25*, 1589−1592.

(3) Mannsfeld, S. C.; Tee, B. C.; Stoltenberg, R. M.; Chen, C. V.; Barman, S.; Muir, B. V.; Sokolov, A. N.; Reese, C.; Bao, Z. Highly sensitive flexible pressure sensors with microstructured rubber dielectric layers. *Nat. Mater.* **2010**, *9*, 859−864.

(4) Lipomi, D. J.; Vosgueritchian, M.; Tee, B. C.; Hellstrom, S. L.; Lee, J. A.; Fox, C. H.; Bao, Z. Skin-like pressure and strain sensors based on transparent elastic films of carbon nanotubes. *Nat. Nanotechnol.* **2011**, *6*, 788−792.

(5) Schwartz, G.; Tee, B. C.-K.; Mei, J.; Appleton, A. L.; Kim, D. H.; Wang, H.; Bao, Z. Flexible polymer transistors with high pressure sensitivity for application in electronic skin and health monitoring. *Nat. Commun.* **2013**, *4*, 1859.

(6) Agarwal, G.; Besuchet, N.; Audergon, B.; Paik, J. Stretchable Materials for Robust Soft Actuators towards Assistive Wearable Devices. *Sci. Rep.* **2016**, *6*, 34224.

(7) Zheng, W.; Alici, G.; Clingan, P. R.; Munro, B. J.; Spinks, G. M.; Steele, J. R.; Wallace, G. G. Polypyrrole stretchable actuators. *J. Polym. Sci., Part B: Polym. Phys.* **2013**, *51*, 57−63.

(8) Ho, D. H.; Sun, Q.; Kim, S. Y.; Han, J. T.; Kim, D. H.; Cho, J. H. Stretchable and Multimodal All Graphene Electronic Skin. *Adv. Mater.* **2016**, *28*, 2601−2608.
(9) Wu, S.; Peng, S.; Wang, C. H. Stretchable strain sensors based on PDMS composites with cellulose sponges containing one- and two-dimensional nanocarbons. *Sens. Actuator A* **2018**, *279*, 90−100.
(10) Zhang, Z.; Ghezawi, N.; Li, B.; Ge, S.; Zhao, S.; Saito, T.; Hun, D.; Cao, P.-F. Autonomous Self-Healing Elastomers with Unprecedented Adhesion Force. *Adv. Funct. Mater.* **2020**, 2006298.
(11) Wu, W. Stretchable electronics: functional materials, fabrication strategies and applications. *Sci. Technol. Adv. Mater.* **2019**, *20*, 187−224.
(12) Odian, G. G., *Principles of polymerization*. 4th ed.; Wiley-Interscience: Hoboken, N.J., 2004; p xxiv, 812 p.
(13) Choong, C.-L.; Shim, M.-B.; Lee, B.-S.; Jeon, S.; Ko, D.-S.; Kang, T.-H.; Bae, J.; Lee, S. H.; Byun, K.-E.; Im, J.; Jeong, Y. J.; Park, C. E.; Park, J.-J.; Chung, U.-I. Highly Stretchable Resistive Pressure Sensors Using a Conductive Elastomeric Composite on a Micropyramid Array. *Adv. Mater.* **2014**, *26*, 3451−3458.
(14) Lai, Y.-C.; Deng, J.; Liu, R.; Hsiao, Y.-C.; Zhang, S. L.; Peng, W.; Wu, H.-M.; Wang, X.; Wang, Z. L. Actively Perceiving and Responsive Soft Robots Enabled by Self-Powered, Highly Extensible, and Highly Sensitive Triboelectric Proximity- and Pressure-Sensing Skins. *Adv. Mater.* **2018**, *30*, 1801114.
(15) Kim, T.; Cho, M.; Yu, K. Flexible and Stretchable Bio-Integrated Electronics Based on Carbon Nanotube and Graphene. *Materials* **2018**, *11*, 1163.
(16) Boaretto, N.; Almenara, J.; Mikhalchan, A.; Marcilla, R.; Vilatela, J. J. A Route to High-Toughness Battery Electrodes. *ACS Appl. Energy Mater.* **2019**, *2*, 5889−5899.
(17) Chen, Q.; Yan, X.; Zhu, L.; Chen, H.; Jiang, B.; Wei, D.; Huang, L.; Yang, J.; Liu, B.; Zheng, J. Improvement of Mechanical Strength and Fatigue Resistance of Double Network Hydrogels by Ionic Coordination Interactions. *Chem. Mater.* **2016**, *28*, 5710−5720.
(18) Saborío, M. C. G.; Lanzalaco, S.; Fabregat, G.; Puiggalí, J.; Estrany, F.; Alemán, C. Flexible Electrodes for Supercapacitors Based on the Supramolecular Assembly of Biohydrogel and Conducting Polymer. *J. Phys. Chem. C* **2018**, *122*, 1078−1090.
(19) Liu, J.; Sheina, E.; Kowalewski, T.; McCullough, R. D. Tuning the Electrical Conductivity and Self-Assembly of Regioregular Polythiophene by Block Copolymerization: Nanowire Morphologies in New Di- and Triblock Copolymers. *Angew. Chem., Int. Ed.* **2002**, *41*, 329−332.
(20) Yu, Z.; Niu, X.; Liu, Z.; Pei, Q. Intrinsically stretchable polymer light-emitting devices using carbon nanotube-polymer composite electrodes. *Adv. Mater.* **2011**, *23*, 3989−3994.
(21) Cao, P. F.; Li, B.; Hong, T.; Xing, K.; Voylov, D. N.; Cheng, S.; Yin, P.; Kisliuk, A.; Mahurin, S. M.; Sokolov, A. P.; Saito, T. Robust and Elastic Polymer Membranes with Tunable Properties for Gas Separation. *ACS Appl. Mater. Interfaces* **2017**, *9*, 26483−26491.
(22) Xu, S.; Zhang, Y.; Cho, J.; Lee, J.; Huang, X.; Jia, L.; Fan, J. A.; Su, Y.; Su, J.; Zhang, H.; Cheng, H.; Lu, B.; Yu, C.; Chuang, C.; Kim, T.-i.; Song, T.; Shigeta, K.; Kang, S.; Dagdeviren, C.; Petrov, I.; Braun, P. V.; Huang, Y.; Paik, U.; Rogers, J. A. Stretchable batteries with self-similar serpentine interconnects and integrated wireless recharging systems. *Nat. Commun.* **2013**, *4*, 1543.
(23) Wang, C.; Wang, C.; Huang, Z.; Xu, S. Materials and Structures toward Soft Electronics. *Adv. Mater.* **2018**, *30*, 1801368.
(24) Bratton, A. F.; Kim, S.-S.; Ellison, C. J.; Miller, K. M. Thermomechanical and Conductive Properties of Thiol−Ene Poly(ionic liquid) Networks Containing Backbone and Pendant Imidazolium Groups. *Ind. Eng. Chem. Res.* **2018**, *57*, 16526−16536.
(25) Fredlake, C. P.; Crosthwaite, J. M.; Hert, D. G.; Aki, S. N. V. K.; Brennecke, J. F. Thermophysical Properties of Imidazolium-Based Ionic Liquids. *J. Chem. Eng. Data* **2004**, *49*, 954−964.
(26) Sutto, T. E.; De Long, H. C.; Trulove, P. C. Physical Properties of Substituted Imidazolium Based Ionic Liquids Gel Electrolytes. *Z. Naturforsch. A* **2002**, *57*, 839.
(27) Yang, Q.; Zhang, Z.; Sun, X.-G.; Hu, Y.-S.; Xing, H.; Dai, S. Ionic liquids and derived materials for lithium and sodium batteries. *Chem. Soc. Rev.* **2018**, *47*, 2020−2064.
(28) Zhang, P.; Li, M.; Yang, B.; Fang, Y.; Jiang, X.; Veith, G. M.; Sun, X. G.; Dai, S. Polymerized Ionic Networks with High Charge Density: Quasi-Solid Electrolytes in Lithium-Metal Batteries. *Adv. Mater.* **2015**, *27*, 8088−8094.
(29) Lin, B.; Qiu, L.; Lu, J.; Yan, F. Cross-Linked Alkaline Ionic Liquid-Based Polymer Electrolytes for Alkaline Fuel Cell Applications. *Chem. Mater.* **2010**, *22*, 6718−6725.
(30) Wilke, A.; Yuan, J.; Antonietti, M.; Weber, J. Enhanced Carbon Dioxide Adsorption by a Mesoporous Poly(ionic liquid). *ACS Macro Lett.* **2012**, *1*, 1028−1031.
(31) Cowan, M. G.; Gin, D. L.; Noble, R. D. Poly(ionic liquid)/Ionic Liquid Ion-Gels with High "Free" Ionic Liquid Content: Platform Membrane Materials for CO2/Light Gas Separations. *Acc. Chem. Res.* **2016**, *49*, 724−732.
(32) Scovazzo, P.; Kieft, J.; Finan, D.; Koval, C.; DuBois, D.; Noble, R. Gas separations using non-hexafluorophosphate [PF6]− anion supported ionic liquid membranes. *J. Membr. Sci.* **2004**, *238*, 57−63.
(33) Amajjahe, S.; Ritter, H. Supramolecular Controlled Pseudo-LCST Effects of Cyclodextrin-Complexed Poly(ionic liquids). *Macromolecules* **2008**, *41*, 3250−3253.
(34) Yoshimitsu, H.; Kanazawa, A.; Kanaoka, S.; Aoshima, S. Well-Defined Polymeric Ionic Liquids with an Upper Critical Solution Temperature in Water. *Macromolecules* **2012**, *45*, 9427−9434.
(35) Xiong, Y.; Wang, H.; Wang, R.; Yan, Y.; Zheng, B.; Wang, Y. A facile one-step synthesis to cross-linked polymeric nanoparticles as highly active and selective catalysts for cycloaddition of CO2 to epoxides. *Chem. Commun.* **2010**, *46*, 3399−3401.
(36) Xiong, Y.; Wang, Y.; Wang, H.; Wang, R.; Cui, Z. Novel one-step synthesis to cross-linked polymeric nanoparticles as highly active and selective catalysts for cycloaddition of CO2 to epoxides. *J. Appl. Polym. Sci.* **2012**, *123*, 1486−1493.
(37) Zhou, T.; Gao, X.; Dong, B.; Sun, N.; Zheng, L. Poly(ionic liquid) hydrogels exhibiting superior mechanical and electrochemical properties as flexible electrolytes. *J. Mater. Chem. A* **2016**, *4*, 1112−1118.
(38) Rhoades, T. C.; Wistrom, J. C.; Daniel Johnson, R.; Miller, K. M. Thermal, mechanical and conductive properties of imidazolium-containing thiol-ene poly(ionic liquid) networks. *Polymer* **2016**, *100*, 1−9.
(39) Tang, J.; Tang, H.; Sun, W.; Radosz, M.; Shen, Y. Low-pressure CO_2 sorption in ammonium-based poly(ionic liquid)s. *Polymer* **2005**, *46*, 12460−12467.
(40) Shao, Y.; Jiang, Z.; Zhang, Y.; Wang, T.; Zhao, P.; Zhang, Z.; Yuan, J.; Wang, H. All-Poly(ionic liquid) Membrane-Derived Porous Carbon Membranes: Scalable Synthesis and Application for Photothermal Conversion in Seawater Desalination. *ACS Nano* **2018**, *12*, 11704−11710.
(41) Weinhold, F.; West, R. The Nature of the Silicon−Oxygen Bond. *Organometallics* **2011**, *30*, 5815−5824.
(42) Fragiadakis, D.; Pissis, P.; Bokobza, L. Glass transition and molecular dynamics in poly(dimethylsiloxane)/silica nanocomposites. *Polymer* **2005**, *46*, 6001−6008.
(43) Jeong, S. H.; Zhang, S.; Hjort, K.; Hilborn, J.; Wu, Z. PDMS-Based Elastomer Tuned Soft, Stretchable, and Sticky for Epidermal Electronics. *Adv. Mater.* **2016**, *28*, 5830−5836.
(44) Liu, H.-S.; Pan, B.-C.; Liou, G.-S. Highly transparent AgNW/PDMS stretchable electrodes for elastomeric electrochromic devices. *Nanoscale* **2017**, *9*, 2633−2639.
(45) Benight, S. J.; Wang, C.; Tok, J. B. H.; Bao, Z. Stretchable and self-healing polymers and devices for electronic skin. *Prog. Polym. Sci.* **2013**, *38*, 1961−1977.
(46) Chen, M.; Tao, T.; Zhang, L.; Gao, W.; Li, C. Highly conductive and stretchable polymer composites based on graphene/MWCNT network. *Chem. Commun.* **2013**, *49*, 1612−1614.
(47) Cao, P.-F.; Naguib, M.; Du, Z.; Stacy, E.; Li, B.; Hong, T.; Xing, K.; Voylov, D. N.; Li, J.; Wood, D. L., III; Sokolov, A. P.; Nanda, J.;

https://dx.doi.org/10.1021/acs.macromol.0c02335
Macromolecules 2021, 54, 896−905

Saito, T. Effect of Binder Architecture on the Performance of Silicon/Graphite Composite Anodes for Lithium Ion Batteries. *ACS Appl. Mater. Interfaces* **2018**, *10*, 3470−3478.
(48) Long, L.; Wang, S.; Xiao, M.; Meng, Y. Polymer electrolytes for lithium polymer batteries. *J. Mater. Chem. A* **2016**, *4*, 10038−10069.
(49) Bocharova, V.; Wojnarowska, Z.; Cao, P. F.; Fu, Y.; Kumar, R.; Li, B.; Novikov, V. N.; Zhao, S.; Kisliuk, A.; Saito, T.; Mays, J. W.; Sumpter, B. G.; Sokolov, A. P. Influence of Chain Rigidity and Dielectric Constant on the Glass Transition Temperature in Polymerized Ionic Liquids. *J. Phys. Chem. B* **2017**, *121*, 11511−11519.
(50) Hong, T.; Cao, P.-F.; Zhao, S.; Li, B.; Smith, C.; Lehmann, M.; Erwin, A. J.; Mahurin, S. M.; Venna, S. R.; Sokolov, A. P.; Saito, T. Tailored CO_2-philic Gas Separation Membranes via One-Pot Thiol−ene Chemistry. *Macromolecules* **2019**, *52*, 5819−5828.
(51) Faucher, J. A.; Koleske, J. V.; Santee, E. R., Jr.; Stratta, J. J.; Wilson, C. W., III Glass Transitions of Ethylene Oxide Polymers. *J. Appl. Phys.* **1966**, *37*, 3962−3964.
(52) Lu, Y.; Hu, Y.; Wang, Z. M.; Manias, E.; Chung, T. C. Synthesis of new amphiphilic diblock copolymers containing poly(ethylene oxide) and poly(α-olefin). *J. Polym. Sci., Part A: Polym. Chem.* **2002**, *40*, 3416−3425.
(53) Lu, X.; Weiss, R. A. Relationship between the glass transition temperature and the interaction parameter of miscible binary polymer blends. *Macromolecules* **1992**, *25*, 3242−3246.
(54) Cao, P.-F.; Li, B.; Yang, G.; Zhao, S.; Townsend, J.; Xing, K.; Qiang, Z.; Vogiatzis, K. D.; Sokolov, A. P.; Nanda, J.; Saito, T. Elastic Single-Ion Conducting Polymer Electrolytes: Toward a Versatile Approach for Intrinsically Stretchable Functional Polymers. *Macromolecules* **2020**, *53*, 3591−3601.
(55) Abraham, K. M.; Jiang, Z.; Carroll, B. Highly Conductive PEO-like Polymer Electrolytes. *Chem. Mater.* **1997**, *9*, 1978−1988.
(56) Zhao, C.-Z.; Zhang, X.-Q.; Cheng, X.-B.; Zhang, R.; Xu, R.; Chen, P.-Y.; Peng, H.-J.; Huang, J.-Q.; Zhang, Q. An anion-immobilized composite electrolyte for dendrite-free lithium metal anodes. *Proc. Natl. Acad. Sci. U. S. A.* **2017**, *114*, 11069−11074.
(57) Xing, K.; Tress, M.; Cao, P.-F.; Fan, F.; Cheng, S.; Saito, T.; Sokolov, A. P. The Role of Chain-End Association Lifetime in Segmental and Chain Dynamics of Telechelic Polymers. *Macromolecules* **2018**, *51*, 8561−8573.
(58) Yamaguchi, M. Rheological properties of linear and crosslinked polymer blends: Relation between crosslink density and enhancement of elongational viscosity. *J. Polym. Sci., Part B: Polym. Phys.* **2001**, *39*, 228−235.
(59) Zarca, G.; Horne, W. J.; Ortiz, I.; Urtiaga, A.; Bara, J. E. Synthesis and gas separation properties of poly(ionic liquid)-ionic liquid composite membranes containing a copper salt. *J. Membr. Sci.* **2016**, *515*, 109−114.
(60) Gorce, J. N.; Hellgeth, J. W.; Ward, T. C. Mechanical hysteresis of a polyether polyurethane thermoplastic elastomer. *Polym. Eng. Sci.* **1993**, *33*, 1170−1176.
(61) Lunkenheimer, P.; Kastner, S.; Köhler, M.; Loidl, A. Temperature development of glassyα-relaxation dynamics determined by broadband dielectric spectroscopy. *Phys. Rev. E* **2010**, *81*, No. 051504.
(62) Stacy, E. W.; Gainaru, C. P.; Gobet, M.; Wojnarowska, Z.; Bocharova, V.; Greenbaum, S. G.; Sokolov, A. P. Fundamental Limitations of Ionic Conductivity in Polymerized Ionic Liquids. *Macromolecules* **2018**, *51*, 8637−8645.
(63) Kisliuk, A.; Bocharova, V.; Popov, I.; Gainaru, C.; Sokolov, A. P. Fundamental parameters governing ion conductivity in polymer electrolytes. *Electrochim. Acta* **2019**, *299*, 191−196.
(64) Leys, J.; Rajesh, R. N.; Menon, P. C.; Glorieux, C.; Longuemart, S.; Nockemann, P.; Pellens, M.; Binnemans, K. Influence of the anion on the electrical conductivity and glass formation of 1-butyl-3-methylimidazolium ionic liquids. *J. Chem. Phys.* **2010**, *133*, No. 034503.
(65) Choudhury, S.; Saha, T.; Naskar, K.; Stamm, M.; Heinrich, G.; Das, A. A highly stretchable gel-polymer electrolyte for lithium-sulfur batteries. *Polymer* **2017**, *112*, 447−456.
(66) Vollas, A.; Chouliaras, T.; Deimede, V.; Ioannides, T.; Kallitsis, J. New Pyridinium Type Poly(Ionic Liquids) as Membranes for CO_2 Separation. *Polymer* **2018**, *10*, 912.
(67) Dai, Z.; Ansaloni, L.; Deng, L. Recent advances in multi-layer composite polymeric membranes for CO2 separation: A review. *Green Energy Environ.* **2016**, *1*, 102−128.
(68) Bara, J. E.; Gin, D. L.; Noble, R. D. Effect of Anion on Gas Separation Performance of Polymer−Room-Temperature Ionic Liquid Composite Membranes. *Ind. Eng. Chem. Res.* **2008**, *47*, 9919−9924.
(69) Lin, H.; Freeman, B. D. Gas solubility, diffusivity and permeability in poly(ethylene oxide). *J. Membr. Sci.* **2004**, *239*, 105−117.
(70) Robeson, L. M. The upper bound revisited. *J. Membr. Sci.* **2008**, *320*, 390−400.

https://dx.doi.org/10.1021/acs.macromol.0c02335
Macromolecules 2021, 54, 896−905